




# Development of a Point-of-Care Test Based on Selenium Nanoparticles for Heart-Type Fatty Acid-Binding Proteins in Human Plasma and Blood

Lanju Wang<sup>1,2,\*</sup>, Mengli Wu<sup>2,\*</sup>, Jingjing Ma<sup>2,\*</sup>, Ziwei Ma<sup>2</sup>, Jiahui Liang<sup>2</sup>, Ningya Tao<sup>2,3</sup>, Yangguang Ren<sup>4</sup>, Shujun Shao<sup>1</sup>, Xin Qi<sup>1</sup>, Zhizeng Wang<sup>2</sup>

<sup>1</sup>Department of Blood Transfusion, the Affiliated Tumor Hospital of Zhengzhou University, Zhengzhou, Henan, 450008, People's Republic of China; <sup>2</sup>Joint National Laboratory for Antibody Drug Engineering, Clinical Laboratory of the First Affiliated Hospital, School of Medicine, Henan University, Kaifeng, Henan, 475004, People's Republic of China; <sup>3</sup>Pingyu Health School, Zhumadian, Henan, 463400, People's Republic of China; <sup>4</sup>Breast and Thyroid Surgery, Huaihe Hospital of Henan University, Kaifeng, Henan, 475004, People's Republic of China

\*These authors contributed equally to this work

Correspondence: Xin Qi, Department of Blood Transfusion, the Affiliated Tumor Hospital of Zhengzhou University, Zhengzhou, 450008, People's Republic of China, Tel +86 15038239612, Email zlyyqixin4215@zzu.edu.cn; Zhizeng Wang, Joint National Laboratory for Antibody Drug Engineering, Clinical Laboratory of the First Affiliated Hospital, School of Medicine, Henan University, Kaifeng, Henan, 475004, People's Republic of China, Tel +86 15093628687, Email wzhenzeng@126.com

**Purpose:** A rapid, convenient, cost-effective in-home test method for identifying heart-type fatty acid-binding protein (H-FABP) in plasma and blood by a lateral-flow immunoassay (LFIA) based on selenium nanoparticles (SeNPs) was developed.

**Methods:** SeNPs were synthesized by using L-ascorbic acid to reduce seleninic acid at room temperature and conjugated with an anti-H-FABP monoclonal antibody. The limit of detection, specificity, and stability were measured, and clinical samples were analyzed.

**Results:** The SeNPs were spherical with a diameter of  $39.48 \pm 3.72$  nm and were conjugated successfully with an anti-H-FABP antibody, resulting in a total diameter of  $46.52 \pm 2.95$  nm. The kit was designed for the determination of H-FABP in plasma specimens and whole blood specimens. The limit of detection was 1 ng/mL in plasma and blood, and the results could be determined within 10 min. No cross-reaction occurred with cardiac troponin I, creatine kinase-MB or myoglobin. The kits were stored at 40 °C for up to 30 days without significant loss of activity. The sensitivity was determined to be 100%, the specificity 96.67%, and the overall coincidence rate 97.83%.

**Conclusion:** This SeNP assay kit can conveniently, rapidly, and sensitively detect H-FABP in plasma or blood with a readout of a simple color change visible to the naked eye with no special device, and can be used as an auxiliary means for the early screening of AMI.

**Clinical Trial Registration:** Plasma and blood samples were used under approval from the Experimental Animal Ethics committee of the Joint National Laboratory for Antibody Drug Engineering, Henan University. The clinical trial registration number was HUSOM-2019-047.

**Keywords:** heart-type fatty acid-binding protein, selenium nanoparticle, lateral-flow immunoassay, point-of-care test, blood

## Introduction

Acute myocardial infarction (AMI) is the primary cause of death worldwide and has high morbidity.<sup>1</sup> Data from the World Health Organization (WHO) indicated that AMI causes 30% of global deaths occur yearly and is expected to cause more than 23 million deaths annually by 2030.<sup>2</sup> AMI is a disease in which myocardial necrosis is caused by unstable ischemic syndrome.<sup>3</sup> Myocardial necrosis is an irreversible injury; in the First two hours after chest pain, 85% of the heart is damaged.<sup>4</sup> Moreover, delayed treatment increases the possibility of death.<sup>5</sup> Successful treatment of AMI requires a rapid and early diagnosis of this disease.<sup>6</sup> Therefore, early detection is essential for the treatment and prognosis of AMI. Biomarkers are released during myocardial injury, and a lateral-flow immunoassay (LFIA) can be used as a point-of-care test for markers.

Many biomarkers are used to diagnose AMI, such as myoglobin (Myo), creatine kinase-Mb (CK-MB), cardiac troponin, and human heart-type fatty acid binding protein (H-FABP).<sup>7-9</sup> Myo is rather sensitive and is elevated within approximately 3 h after AMI. However, Myo is not specific to cardiac injury, and other muscle injuries also release Myo into the blood.<sup>8</sup> Although CK-MB has a wide range of clinical applications, it has general specificity, especially for AMI, within 6 h.<sup>10</sup> Although the specificity is high, this marker is used mainly for the diagnosis of myocardial infarction with a recurrent attack in a short time period due to its short duration.<sup>7,11</sup> cTnT and cTnI have high specificity, particularly the appearance of hs-cTnI, but they are limited by the sensitivity of current rapid detection technology; thus, these biomarkers cannot be detected with home detection methods. H-FABP, which is related to fatty acid metabolism, is a cytoplasmic protein with a low molecular weight of 14 kDa to 15 kDa.<sup>12</sup> This novel biomarker was shown to be released into the circulation following myocardial necrosis.<sup>13</sup> H-FABP was first discovered in the 1980s and reported to be released by the injured myocardium.<sup>14</sup> Currently, H-FABP is clinically used as an early cardiac marker of AMI.<sup>10,14,15</sup> The level of H-FABP is significantly elevated above its threshold value within approximately 2 h after the first clinical symptom onset.<sup>16-18</sup> H-FABP is mainly expressed in myocardial tissue rather than skeletal muscle and is a more specific AMI marker than Myo.<sup>18,19</sup> Unfortunately, most current commercial H-FABP assays are chromatographic immunoassays (CIAs), enzyme-linked immunosorbent assays (ELISAs) and LFIA based on colloidal gold.<sup>20-23</sup> CIA and ELISA can achieve quantitative detection, but they require specific equipment and the participation of technicians, which limits the scope of application.<sup>21</sup> Colloidal gold has been widely used in the field of biomarker detection. However, high-temperature boiling is required in its relatively complicated preparation process, and the raw material is relatively expensive. In this study, we used selenium nanoparticles (SeNPs), which are easier to prepare and less expensive than colloidal gold. In addition, SeNPs maintain a stable state in water in the presence of stabilizers, whereas colloidal gold relies on the surface electric double layer to maintain a stable state in water.<sup>24</sup> SeNPs were used as the label to develop a rapid, sensitive,<sup>25</sup> portable LFIA for detecting H-FABP in the plasma and blood of AMI patients. This test strip provides a quick and easy method for the diagnosis of AMI and has good clinical value. It also allows the at-home detection of AMI, similar to blood glucose detection.

## Materials and Methods

### Materials and Apparatus

Recombinant protein (R020201) and monoclonal antibodies (mAb) for capture (M020201, mAb2) and conjugate (M020203, mAb1) were purchased from Biogenome (Hangzhou, China). H-FABP-Free Matrix was obtained from HyTest (Turku, Finland). Bovine serum albumin (BSA) and trehalose were purchased from Sigma Aldrich (St. Louis, USA). Potassium carbonate was purchased from Zhiyuan Chemical Reagent (Tianjin, China). Tween 20 was obtained from Solarbio (Beijing, China). Sucrose was obtained from Sinopharm Chemical Reagents (Shanghai, China). Sodium dodecyl sulfate (SDS) was provided by Aladdin (Shanghai, China). Polyethylene glycol (PEG) was purchased from Yuanye (Shanghai, China). Ascorbic acid (Vc) and selenium acid ( $\text{H}_2\text{SeO}_3$ ) were obtained from Xiya Reagent (Shandong, China). Nitrocellulose membrane HF 135, precision pH test paper and ultrapure water meter were obtained from Millipore (Merck, Germany). The goat anti-mouse IgG, glass fiber, absorbent pad, adhesive backing card, dispenser and sprayer XYZ 3010, guillotine cutter and other experimental supplies were provided by Shanghai Jining Biological Technology Co., Ltd. (Shanghai, China). The BLUE PARD Blast oven was provided by Shanghai YiHeng Scientific Instruments Ltd. (Shanghai, China). VORTEX and LOOPSTER digital were obtained from IKA (Staufen, Germany). The H-FABP ELISA Kit was obtained from Hycult Biotech (Catalog number: HK401; Lot number: 19750K0517-Z).

### Preparation of Selenium Nanoparticles

All of the glassware was siliconized, cleaned in aqua regia [ $\text{HCl}/\text{HNO}_3$  (3 v/v)], and thoroughly washed with ultrapure water before use. All solutions were filtered by a 0.45  $\mu\text{m}$  filter. SeNPs were prepared from selenious acid reduced by ascorbic acid in a soft template composed of sodium diethyl sulfate+polyethylene glycol (SDS+PEG) in ultrapure water.<sup>26-28</sup> Briefly, 20 mL of 2.27 M PEG was added to 140 mL of deionized water and continuously stirred for 10 min. Then, 20 mL of 0.1 M SDS, 10 mL of 0.64 M ascorbic acid and 10 mL of 0.08 M  $\text{H}_2\text{SeO}_3$  were added step by step with 15 min of mixing per stage to allow

the reaction to complete. All reactions were carried out with agitation at room temperature (RT). The SeNPs were characterized by transmission electron microscopy (TEM) and dynamic light scattering (DLS).<sup>29–32</sup>

## Preparation of H-FABP Specific SeNP Conjugate

The pH of SeNPs was adjusted by  $K_2CO_3$ , and different concentrations of mAb1 were conjugated with SeNPs for 30 min at RT. Then, BSA was added to the mixture to block the active site of SeNPs via a physical adsorption reaction to reach a final BSA concentration of 1% for 30 min at RT. The prepared specific conjugates were centrifuged at 10,000 rpm for 20 min at 4 °C, the supernatant was discarded, and the precipitate was finally dispersed in a storage solution (10 mM PBS, containing 10% bovine serum, 1% Tween-20, 10% sucrose, 5% trehalose, 0.5% BSA)<sup>33</sup> and stored at 4 °C.<sup>34</sup>

## Assembly of the H-FABP Test Strip Based on SeNPs

The assembly of the LFIA was described previously.<sup>35,36</sup> The structure and assembly of the LFIA strip are shown in Figure 1A. The sample pad, conjugate pad, nitrocellulose membrane (NC membrane), and absorbent pad were assembled on a PVC plate in turn. A sandwich method was adopted to establish the H-FABP test strip.

The conjugate pad was coated with SeNP-anti-H-FABP mAb 1, while the test line (T) and control lines (C) on the NC membrane were coated with anti-H-FABP mAb2 and goat anti-mouse IgG, respectively. Once the sample was dropped onto the sample pad, the conjugate was reconstituted and chromatographed toward the absorbent pad. If the sample was positive, H-FABP bound to the SeNP-anti-H-FABP mAb1 on the conjugate pad and continued to move to the T and C of the NC membrane. On the T, it bound to anti-H-FABP mAb2, forming a SeNPs-mAb1-H-FABP-mAb2 complex. The aggregated molecules displayed an orange color at the T. SeNP-anti-H-FABP mAb1 that was not combined with H-FABP continued to move to the C. At the C, SeNP-anti-H-FABP mAb1 bound with goat anti-mouse IgG, and the aggregated molecules also showed an orange color. When the T and C simultaneously showed an orange color, the test was considered to be positive; it was negative when only the C displayed an orange color; and when the T and C showed no color or only the T showed an orange color, the result was judged invalid (Figure 1B).

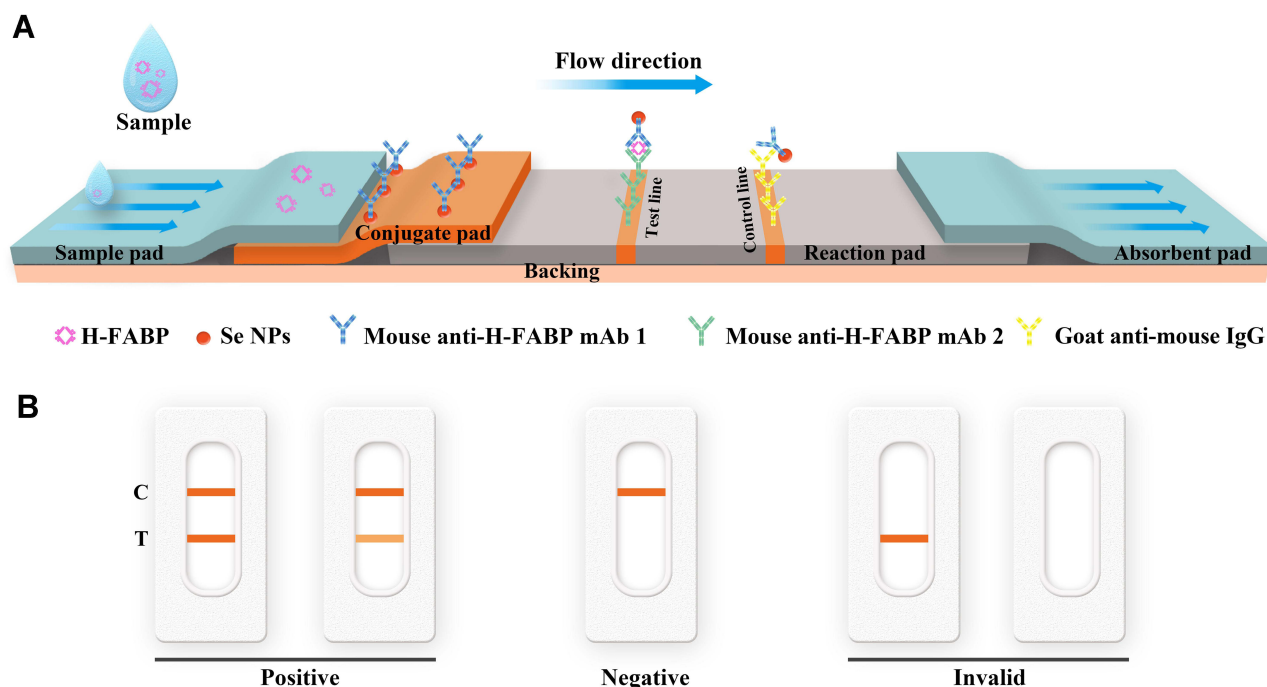


**Figure 1** Diagram and components of the lateral flow immunoassay test strip for H-FABP (A) and visual assessment guidelines for interpreting the test strip results (B). **Abbreviations:** H-FABP: Heart-type fatty acid binding protein; C: Control line; T: Test line.

Before installing the LFIA, the buffer compositions of the sample pad, SeNps-mAb1 levels and antibody amounts for T and C were optimized to maximize the test effectiveness.

1. Sample pad. Glass fiber pads cut to a size of 2.2 cm\*20 cm were dipped in phosphate buffer containing 5% bovine serum and 1% Tween-20 for 5 min. After 2 h of drying at 40 °C, the sample pads above were stored in a blast oven.
2. Reaction pad. The NC membrane was tailored to a 2.5 cm\*20 cm reaction pad. The mAb2 and goat anti-mouse IgG were coated to form the test line and control line, respectively. The diluted antibodies were dispensed by a dispenser and sprayer to the NC membranes at 0.8 µL/cm to form T and C, respectively. After drying for 4 h at 40 °C, the NC membrane was sealed and stored in a blast oven at 40 °C with a humidity of approximately 30% RH.
3. Conjugate pad. The conjugate pad was made of glass fiber cut to 2.5 cm\*20 cm. The conjugate complex was sprayed on the glass fiber to prepare the conjugate pad. After 6 h of drying at 40 °C, the prepared conjugate pads were stored in a blast oven until use.
4. Absorbent pad. An absorbent pad (absorbent paper) was cut to a size of 1.7 cm\*20 cm, and no pretreatment was needed. The function of the absorbent pad was to ensure the rapid progress of the reaction.

The assembled system was cut into 4 mm-wide strips by a guillotine cutter for detection studies.

## Limit of Detection, Specificity, Stability and Recovery Experiment of the H-FABP Test Kit

The H-FABP recombinant protein was diluted with H-FABP-free serum to obtain samples of different concentrations. Eighty microliters of each sample was added to the sample pad for sensitivity detection. CK-MB, cTnI and Myo were added to H-FABP-free serum separately for specificity research. The kits were stored at 4 °C, 25 °C and 40 °C for 30 days, and validity was assessed monthly. The test result was determined by the intensity of the T line, which was easily observed by the naked eye. Each test result was interpreted by 3 different people using ImageJ and plotted by GraphPad Prism.

Two concentrations of H-FABP were detected for the recovery experiment by an ELISA kit. Each concentration test was repeated at least three times, and the SD value and CV% were calculated by SPSS.

## Clinical Serum Sample Detection

Clinical specimens, including the plasma and blood of confirmed positive and negative patients, were applied to the LFIA assay using ELISA as the contrast method. We confirmed that all specimen donors gave informed consent. The sensitivity, specificity, positive predictive value, and negative predictive value of the kit were calculated according to the following formulas:<sup>27</sup>

$$\text{Sensitivity} = [\text{true positive}/(\text{true positive} + \text{false negative})] \times 100\%$$

$$\text{Specificity} = [\text{true negative}/(\text{true negative} + \text{false positive})] \times 100\%$$

## Results and Discussion

### Characterization of Selenium Nanoparticles

The SeNPs formed a clear and bright colloidal solution. After centrifugation, the supernatant was transparent, and the SeNPs could be resuspended well (Figure 2A). TEM showed that the SeNPs were spherical, uniform nanocomposites  $39.48 \pm 3.72$  nm in diameter (Figure 2B). Analysis of the particle size distribution and stability (Figure 2C) and zeta electric potential (ZP) (Figure 2D) showed that the SeNps were prepared with good dispersion and stability, with a polydispersity index (PDI) of 0.038 and a ZP value of -18.6 mV. The SeNPs were placed at the bottom of the centrifuge tube after centrifugation. When the tube was placed flat, the sediment gradually spread out, indicating that the

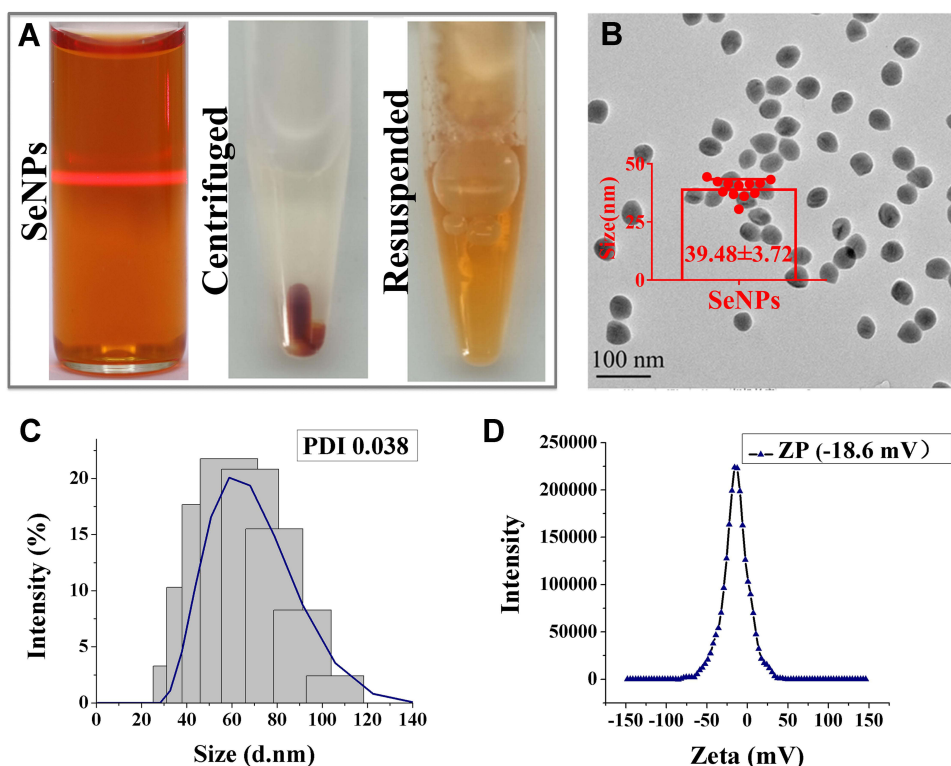


**Figure 2** Characterization of SeNPs: **(A)** images of SeNPs, SeNPs after centrifugation, and SeNPs after suspension. **(B)** TEM result of SeNPs, **(C)** PDI result and **(D)** ZP result of SeNPs by DLS.

**Abbreviations:** SeNPs: Selenium nanoparticles; TEM: Transmission electron microscopy; DLS: Dynamic light scattering; PDI: Polymer dispersity index; ZP: Zeta potential.

SeNPs were not agglomerated. The Se NPs are orange, and the color is not affected by the type and dosage of stabilizer, and the theoretical absorption wavelength range is 480–500 nm, but the Se NPs only showed an absorption peak at 265 nm, which indicated the reducing effect of L-ascorbic acid. Therefore, the absorption peak of Se NPs could not be determined from 400–500 nm due to the strong absorbance of L-ascorbic acid overlapping with the spectra of Se NPs according to our previous study.<sup>37</sup> Se NPs have superior biocompatibility and antioxidant properties and can be conjugated with antibodies or proteins based on hydrogen bonding, hydrophobic interactions, and van der Waals forces.<sup>24,38</sup> In addition, SeNPs are insensitive to salt ions and are suitable for labeling proteins that can be dissolved in high-salt systems.

## Preparation of Selenium Nanoparticle-mAb Conjugate

Each protein has a specific isoelectric point (pI). The pI of the anti-H-FABP mAb is 5.1.<sup>12</sup> The adsorption of protein by nanoparticles depends mainly on the pH of their environment. They combine easily to form a nanoparticle-protein conjugate when the environment is close to or slightly above the pI of the protein.<sup>39</sup> SeNPs and protein conjugate by physical adsorption, and the pH affects the binding efficiency. The SeNP-conjugated mAb1 complex was spherical with a diameter of  $46.52 \pm 2.95$  nm, as determined by TEM (Figure 3A). The average hydrated diameters of the SeNPs and complex were 66.11 nm and 79.60 nm, respectively, with 0.022 and 0.070 PDI values by DLS, respectively (Figure 3B). pH values of 6.5, 7.0 and 7.5 were selected to assess the binding effect of SeNPs and mAb1. According to the color rendering on the test line, control line and reaction pad background, the reaction effect of the kit with pH 7.0 was better than that of other groups with pH 6.5 and pH 7.5 (Figure 3C). The full results of the pH selected assay are shown in Supplemental Figure 1, and pH 7.0 was chosen for the next experiment.

The sensitivity and stability of the kits were adjusted by the conjugate concentration of SeNPs with mAb1. Different concentrations of mAb1 from 4 µg/mL to 6 µg/mL were used for labeling at a pH of 7.0. The kits labeled with 5 µg/mL



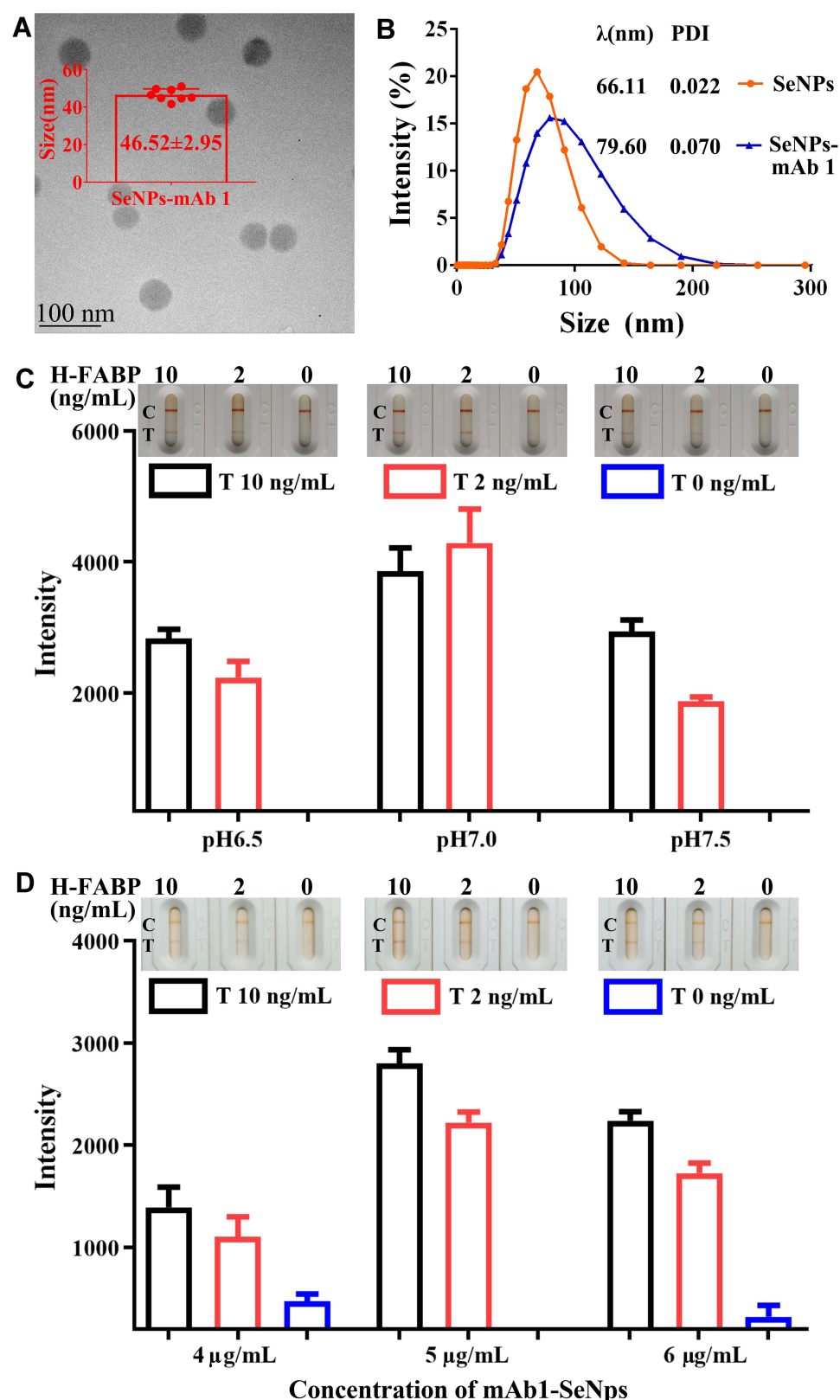


**Figure 3** Characterisation, optimal pH and labelling concentration of the SeNPs-anti-H-FABP mAb1. TEM (A) and DLS (B) result of SeNPs-anti-H-FABP mAb; Detection results and auxiliary judgement result (C) with H-FABP kit at different pH values; Detection results and auxiliary judgement result (D) with H-FABP kit at different concentrations of mAb1.

**Abbreviations:** SeNPs: Selenium nanoparticles; H-FABP: Heart-type fatty acid binding protein; mAb: Monoclonal antibody; TEM: Transmission electron microscopy; DLS: Dynamic light scattering; PDI: Polymer dispersity index; C: Control line; T: Test line.

antibodies showed better results than those of the 4  $\mu\text{g/mL}$  group, which displayed poor sensitivity, and weak false positive results were observed in the 6  $\mu\text{g/mL}$  group (Figure 3D). The full results of the mAb1 concentration selected assay are shown in Supplemental Figure 2. We finally decided that 5  $\mu\text{g/mL}$  was the optimal labeling concentration. The conjugation was stable according to the PDI value by DLS using pH values of 7.0 and 5  $\mu\text{g/mL}$  and according to the conditions used to carry out the characteristic kit experiment. The capture concentration of mAb2 on the test line was 1 mg/mL, and the result is shown in Supplemental Figure 3.

## Limit of Detection, Specificity and Stability of the H-FABP Test Strip

The limit of detection (LOD) and specificity of the kit indicate whether the kit can meet the needs of clinical diagnosis. To characterize the sensitivity of the H-FABP kit, we tested H-FABP-free plasma and blood samples spiked with different concentrations of H-FABP. H-FABP (1 mg/mL) was diluted to gradient concentrations and dropped into the sample pad for detection. The kits became colored orange simultaneously at both C and T within 10 min, and the orange intensity of the test lines gradually decreased as the concentration of H-FABP increased from 0 to 10 ng/mL; when the concentration was 1 ng/mL, the test lines were invisible (positive results) to the naked eye. All control lines were clearly visible (Figure 4A). The auxiliary interpretation results by ImageJ and GraphPad Prism are shown in Figure 4B and are consistent with the naked eye results. Therefore, the LOD of the H-FABP kit was 1 ng/mL in plasma. Similarly, H-FABP  $\geq 1$  ng/mL produced positive results on the kit, and the LOD was 1 ng/mL in blood, as detected by the naked eye (Figure 4C) and ImageJ and GraphPad Prism (Figure 4D). All our experimental results were highly repeatable. When testing whole blood, in addition to using sample diluent, a blood filter membrane was added to the sample pad to reduce the influence of red blood cells and other substances in the blood on the immune response.

The analytical specificity of the H-FABP kit was further characterized by testing several common AMI markers, including cTnI, CK-MB and Myo, for other H-FABP assays. The results shown in Figure 5A indicate that samples containing H-FABP displayed an orange color on both C and T. However, when the samples containing cTnI (20 ng/mL),

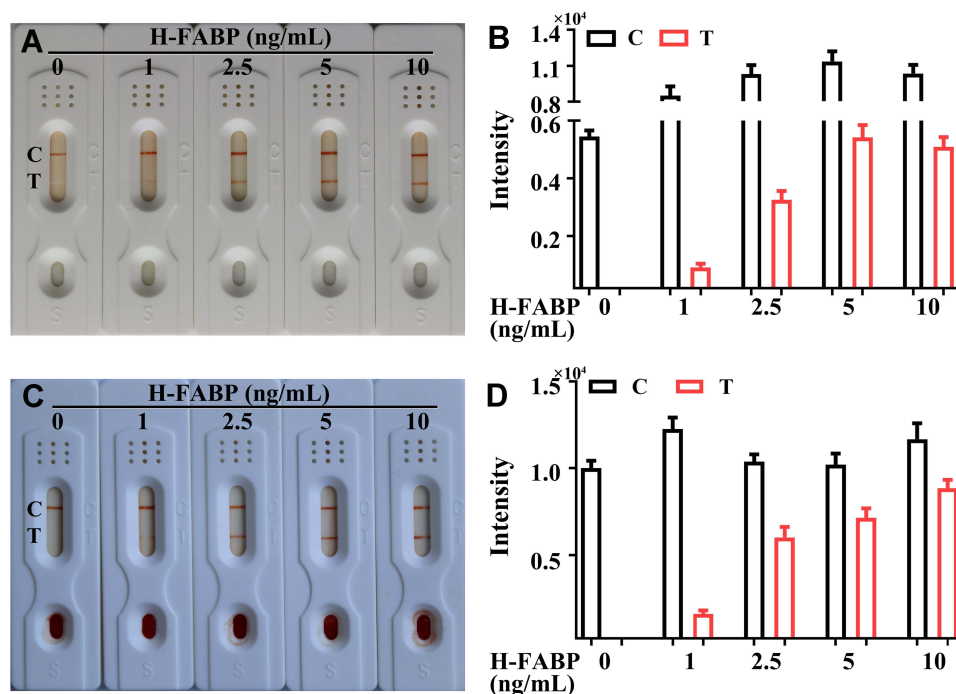


**Figure 4** The limit of detection of the H-FABP kit in plasma and blood. Detection results for H-FABP in plasma observed by the naked eyes (A) and auxiliary interpretation results by ImageJ and GraphPad Prism (B). Detection results for H-FABP in blood observed by the naked eyes (C) and auxiliary interpretation results by ImageJ and GraphPad Prism (D).

**Abbreviations:** H-FABP: Heart-type fatty acid binding protein; C: Control line; T: Test line.

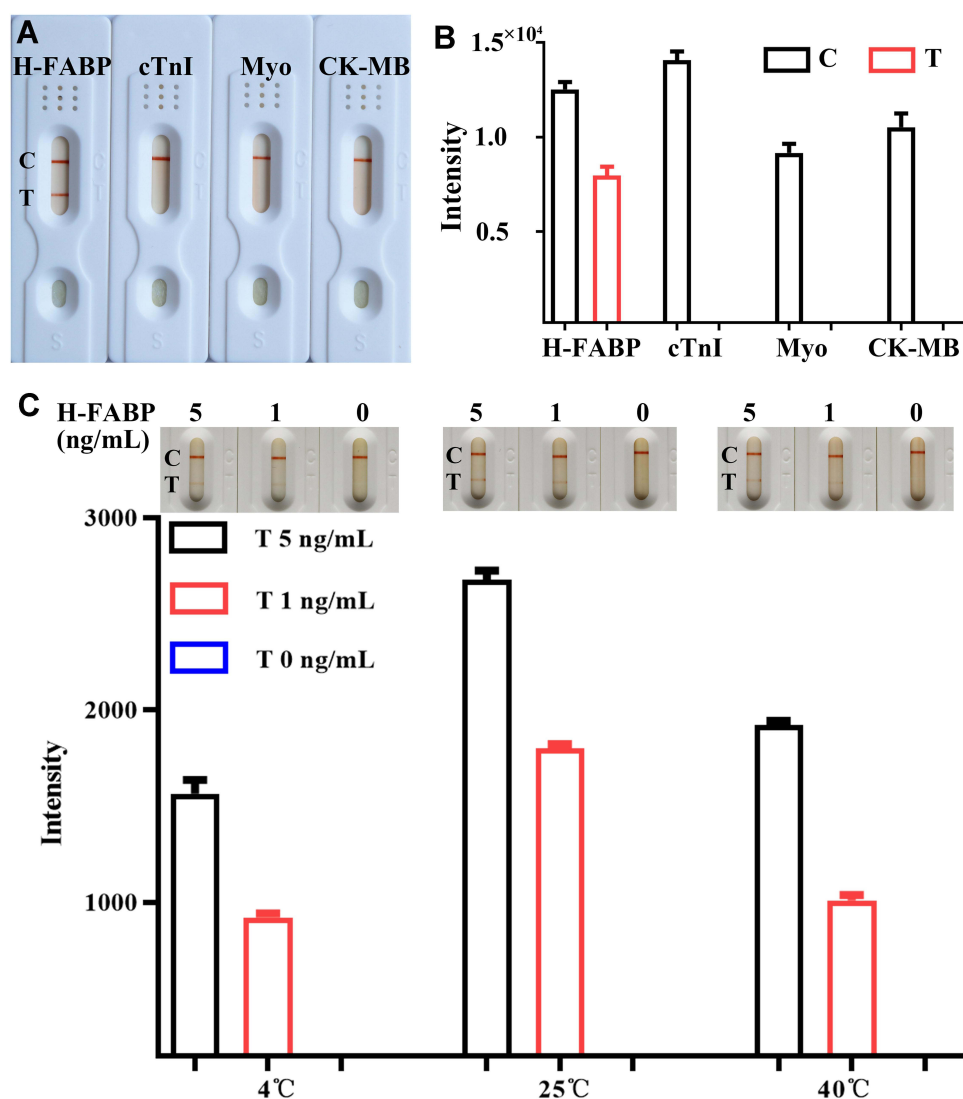


**Figure 5** The specificity and stability of the H-FABP kit. Detection results of specificity for H-FABP observed by the naked eyes (**A**) and auxiliary interpretation results by ImageJ and GraphPad Prism (**B**). Detection results of stability for H-FABP observed by the naked eyes and auxiliary interpretation results by ImageJ and GraphPad Prism (**C**). **Abbreviations:** H-FABP: Heart-type fatty acid binding protein; cTnI: Cardiac troponin I; Myo: Myoglobin; CK-MB: Creatine kinase-Mb; C: Control line; T: Test line.

CK-MB (5 µg/mL) or Myo (5 µg/mL) were tested, the T area on the kits was not colored by the naked eye, and the auxiliary interpretation results were consistent with the naked eye results (Figure 5B). These results suggest that the kit for H-FABP detection has no cross-reactivity with cTnI, CK-MB and Myo, showing good specificity. During the test, it was found that a cross-reaction with ≥ 50 ng/mL cTnI could occur (Supplemental Figure 4), but the clinical cutoff value of cTnI for MI was 1 ng/mL, so this cross-reaction would not affect the interpretation of the results.

**Table 1** Results of Recovery Experiment for H-FABP

Category Standard (ng/mL)		Number of Experiment			Ave	SD	CV (%)
		1	2	3			
H-FABP	0.5	0.4327	0.4541	0.4260	0.4376	0.01468	3.35%
	1.0	0.9323	0.9413	0.8908	1.0674	0.02694	2.92%

**Abbreviations:** H-FABP, heart-type fatty acid binding protein; Ave, average; SD, standard deviation; CV, coefficient of variation.



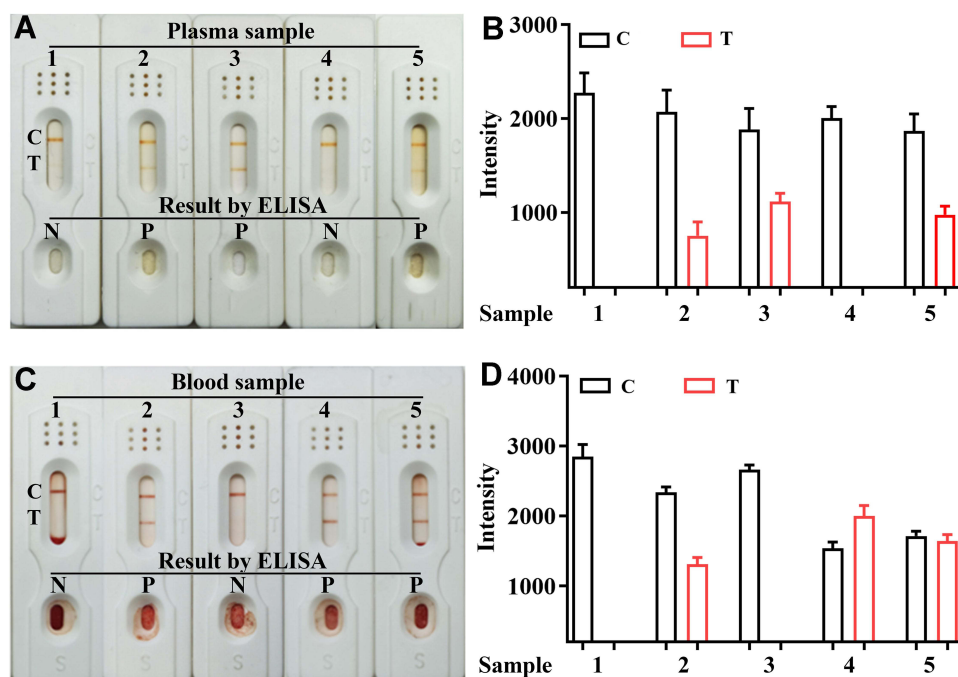


**Figure 6** Detection results of actual samples of this kits for H-FABP in plasma and blood samples. Detection results of plasma for H-FABP observed by the naked eyes (**A**) and auxiliary interpretation results by ImageJ and GraphPad Prism (**B**); Detection results of blood for H-FABP observed by the naked eyes (**C**) and auxiliary interpretation results by ImageJ and GraphPad Prism (**D**).

**Abbreviations:** ELISA: Enzyme linked immunosorbent assay; P: Positive; N: Negative; C: Control line; T: Test line.

To evaluate stability, the same batches of the H-FABP kit were stored at 4 °C, 25 °C and 40 °C for 1 month. Their effectiveness was tested monthly by evaluating the sensitivity. The H-FABP sensitivity under different storage conditions was still 1 ng/mL in H-FABP-free serum, as shown in [Figure 5C](#), by the naked eye, ImageJ and GraphPad Prism. The full results of the stability test are shown in [Supplemental Figure 5](#). Therefore, the LOD of the test kits did not change, indicating outstanding stability. Because the humidity in the Laboratory cannot be controlled, different storage conditions will be present, and the color depth will vary, but this does not affect the sensitivity of the kit. In the next step, we will assess the impact of the same humidity and different temperatures on the kit.

For this purpose, 0.5 ng/mL and 1 ng/mL H-FABP were detected by the H-FABP ELISA kit, with three replicates for each concentration. The SD and CV% values are shown in [Table 1](#). The detection results of the recovery experiment are shown in [Supplemental Table 1](#). H-FABP was calculated according to the fitting curve:  $y \text{ (pg)} = 901.99x^3 - 2488x^2 + 3188.7x - 205.01$ , with  $R^2 = 0.9995$  of [Supplemental Figure 6](#) and [Supplemental Table 2](#).

**Table 2** Distribution of Detection Results for Actual Samples

Experimental Methods	Confirmed by ELISA		
	Positive Samples	Negative Samples	Total Samples
Positive by Se-NPs kit	16	1	17
Negative by Se-NPs kit	0	29	29
Total	16	30	46

**Abbreviations:** Se-NPs, selenium nanoparticles; ELISA, enzyme-linked immunosorbent assay.

## Sandwich Detection of H-FABP in Spiked and Real Samples

The 16 plasma and 30 blood samples collected from the hospital were detected by ELISA and this kit, and the basic information of the samples is shown in [Supplemental Table 3](#) and [Supplemental Table 4](#). The detection results of some samples of plasma and blood are shown in [Figure 6A–D](#), respectively. The results of all samples are shown in [Supplemental Figure 7](#) (plasma) and [Supplemental Figure 8](#) (blood). The sensitivity of the kit was determined to be 100% (16/16), the specificity was 96.67% (29/30), and the overall coincidence rate was 97.83% (45/46) ([Table 2](#)). These results indicate that the established SeNps-LFIA is accurate and suitable for the detection of different substrate samples. However, the color intensity of the test line was not completely consistent with the H-FABP concentration in the sample, which could result from different factors, such as sample hemolysis. In addition, whether the storage time affects the test result also needs to be verified. To fully verify the applicability of this kit, it is still necessary to further expand the amount of clinical samples to.

## Conclusions

This study developed a sensitive SeNps-LFIA for the rapid detection of H-FABP in plasma and blood. The diagnostic strip showed high sensitivity, specificity and stability for detecting H-FABP in plasma and blood samples. The test strip is easy to operate, with a detection limit of 1 ng/mL in both plasma and blood. The easy preparation of nanomaterials and sensitive detection of H-FABP showed potential applicability for real samples. To the best of our knowledge, this is the first report of using SeNps for detecting H-FABP. Additional optimization will be carried out to improve the detection sensitivity.

## Abbreviations

Se-NP, selenium nanoparticle; LFIA, lateral-flow immunoassay; H-FABP, heart-type fatty acid binding protein; AMI, acute myocardial infarction; Myo, myoglobin; CK-MB, creatine kinase-Mb; cTn, cardiac troponin; SDS, sodium dodecyl sulfate; PEG, polyethylene glycol; ELISA, enzyme-linked immunosorbent assay; CIA, chromatographic immunoassay; H<sub>2</sub>SeO<sub>3</sub>, selenous acid; Ab, antibody; mAb, monoclonal antibody; TEM, transmission electron microscopy; DLS, dynamic light scattering; PDI, polymer dispersity index; ZP, zeta potential; IgG, immunoglobulin G; K<sub>2</sub>CO<sub>3</sub>, potassium carbonate; PBS, phosphate-buffered saline; BSA, bovine serum albumin; RH, relative humidity.

## Ethics Statement

We confirmed that all specimen donors gave informed consent, and this study was conducted in compliance with the Declaration of Helsinki.

## Acknowledgments

We thank AJE for linguistic assistance during the preparation of this manuscript.

## Author Contributions

All authors made a significant contribution to the work reported, whether in the conception, study design, execution, acquisition of data, analysis and interpretation, or all these areas; took part in drafting, revising or critically reviewing the article; gave final approval of the version to be published; have agreed on the journal to which the article has been submitted; and agree to be accountable for all aspects of the work.

## Funding

This research was funded by the Science and Technology Department of Henan Province (grant numbers 212102310174 and 222102310079) and the Key Scientific Research Projects of Colleges and Universities in Henan Province (grant numbers 22A320001 and 21A310002).

## Disclosure

The authors declare that they have no competing interests in this work.

## References

- Roth GA, Johnson C, Abajobir A, et al. Global, regional, and national burden of cardiovascular diseases for 10 causes, 1990 to 2015. *J Am Coll Cardiol*. 2017;70(1):1–25. doi:10.1016/j.jacc.2017.04.052
- Fathil MFM, Arshad MKM, Gopinath SCB, et al. Diagnostics on acute myocardial infarction: cardiac troponin biomarkers. *Biosens Bioelectron*. 2015;70:209–220.
- Thygesen K, Alpert JS, Jaffe AS, et al. Third universal definition of myocardial infarction. *J Am Coll Cardiol*. 2012;60:1581–1598.
- Zhang D, Jiang C, Feng Y, et al. Molecular imaging of myocardial necrosis: an updated mini-review. *J Drug Target*. 2020;28(6):565–573.
- Kim K, Park C, Kwon D, et al. Silicon nanowire biosensors for detection of cardiac troponin I (cTnI) with high sensitivity. *Biosens Bioelectron*. 2016;77:695–701.
- Roffi M, Patrono C, Collet J, et al. 2015 ESC Guidelines for the management of acute coronary syndromes in patients presenting without persistent ST-segment elevation. Task force for the management of acute coronary syndromes in patients presenting without persistent ST-segment elevation of the European Society of cardiology (ESC). *G Ital Cardiol*. 2016;17:831–872.
- Shanmugam NR, Muthukumar S, Tanak AS, et al. Multiplexed electrochemical detection of three cardiac biomarkers cTnI, cTnT and BNP using nanostructured ZnO-sensing platform. *Future Cardiol*. 2018;14:131–141.
- Savin M, Mihailescu CM, Matei I, et al. A quantum dot-based lateral flow immunoassay for the sensitive detection of human heart fatty acid binding protein (hFABP) in human serum. *Talanta*. 2018;178:910–915.
- Fan J, Ma J, Xia N, et al. Clinical value of combined detection of CK-MB, MYO, cTnI and plasma NT-proBNP in diagnosis of acute myocardial infarction. *Clin Lab*. 2017;63:427–433.
- Kleine AH, Glatz JFC, Van Nieuwenhoven FA, et al. Release of heart fatty acid-binding protein into plasma after acute myocardial infarction in man. *Mol Cell Biochem*. 1992;116:155–162.
- Shanmugam NR, Muthukumar S, Chaudhry S, et al. Ultrasensitive nanostructure sensor arrays on flexible substrates for multiplexed and simultaneous electrochemical detection of a panel of cardiac biomarkers. *Biosens Bioelectron*. 2017;89:764–772.
- Ren YG, Liu MC, Ji MZ, et al. Rapid detection of human heart-type fatty acid-binding protein in human plasma and blood using a colloidal gold-based lateral flow immunoassay. *Exp Ther Med*. 2021;22(5):1238.
- Otaki Y, Watanabe T, Kubota I. Heart-type fatty acid-binding protein in cardiovascular disease: a systemic review. *Clin Chim Acta*. 2017;474:44–53.
- Glatz JFC, van Bilsen M, Paulussen RJA, et al. Release of fatty acid-binding protein from isolated rat heart subjected to ischemia and reperfusion or to the calcium paradox. *Biochim Biophys Acta*. 1988;961:148–152.
- Adams JE, Abendschein DR, Jaffe AS. Biochemical markers of myocardial injury. Is MB creatine kinase the choice for the 1990s? *Circulation*. 1993;88:750–763.
- Kabekkodu SP, Mananje SR, Saya RP. A study on the role of heart type fatty acid binding protein in the diagnosis of acute myocardial infarction. *J Clin Diagn Res*. 2016;10:OC07–OC10.
- Vupputuri A, Sekhar S, Krishnan S, et al. Heart-type fatty acid-binding protein (H-FABP) as an early diagnostic biomarker in patients with acute chest pain. *Indian Heart J*. 2015;67:538–542.
- Pyati AK, Devaranavadagi BB, Sajjannar SL, et al. Heart-type fatty acid binding protein: a better cardiac biomarker than CK-MB and myoglobin in the early diagnosis of acute myocardial infarction. *J Clin Diagn Res*. 2015;9:BC08–BC11.
- Pyati AK, Devaranavadagi BB, Sajjannar SL, et al. Heart-type fatty acid-binding protein, in early detection of acute myocardial infarction: comparison with CK-MB, troponin I and myoglobin. *Indian J Clin Biochem*. 2016;31:439–445.
- Valle HA, Riesgo LGC, Bel MS, et al. Clinical assessment of heart-type fatty acid binding protein in early diagnosis of acute coronary syndrome. *Eur J Emerg Med*. 2008;15:140–144.
- Shabaiek A, Ismael NEH, Elsheikh S, et al. Role of cardiac myocytes heart fatty acid binding protein depletion (H-FABP) in early myocardial infarction in human heart (autopsy study). *Open Access Maced J Med Sci*. 2016;4:17–21.
- Van Hise CB, Greenslade JH, Parsonage W, et al. External validation of heart-type fatty acid binding protein, high-sensitivity cardiac troponin, and electrocardiography as rule-out for acute myocardial infarction. *Clin Biochem*. 2018;52:161–163.
- Bank IEM, Dekker MS, Hoes AW, et al. Suspected acute coronary syndrome in the emergency room: limited added value of heart type fatty acid binding protein point of care or ELISA tests: the FAME-ER (fatty acid binding protein in myocardial infarction evaluation in the emergency room) study. *Eur Heart J Acute Cardiovasc Care*. 2015;5:364–374.
- Wang Z, Zhou Q, Guo Y, et al. Rapid detection of ractopamine and salbutamol in swine urine by immunochromatography based on selenium nanoparticles. *Int J Nanomed*. 2021;16:2059–2070.
- Wang Z, Jing J, Ren Y, et al. Preparation and application of selenium nanoparticles in a lateral flow immunoassay for clenbuterol detection. *Mater Lett*. 2019;234:212–215.
- Zhang J, Teng Z, Yuan Y, et al. Development, physicochemical characterization and cytotoxicity of selenium nanoparticles stabilized by beta-lactoglobulin. *Int J Biol Macromol*. 2018;107:1406–1413.
- Niu MY, Fang Y, Gu WY. Synthesis of Selenium nanospheres using SDS-PEG cluster as soft template. *J Jiangnan Univ*. 2011;10:67–71.
- Kong H, Yang J, Zhang Y, et al. Synthesis and antioxidant properties of gum arabic-stabilized selenium nanoparticles. *Int J Biol Macromol*. 2014;65:155–162.
- Syed A, Ahmad A. Extracellular biosynthesis of CdTe quantum dots by the fungus *Fusarium oxysporum* and their anti-bacterial activity. *Spectrochim acta A*. 2013;106:41–47.

30. Senapati S, Syed A, Khan S, et al. Extracellular biosynthesis of metal sulfide nanoparticles using the fungus *Fusarium oxysporum*. *Curr Nanosci*. 2014;10(4):588–595.
31. Syed A, Al Saedi MH, Bahkali AH, et al.  $\alpha$ Au 2 S nanoparticles: fungal-mediated synthesis, structural characterization and bioassay. *Green Chem Lett Rev*. 2022;15(1):59–68.
32. Syed A, Al Saedi MH, Bahkali AH, et al. Biological synthesis of  $\alpha$ -Ag<sub>2</sub>S composite nanoparticles using the fungus *Humicola* sp. and its biomedical applications. *J Drug Deliv Sci Tec*. 2021;22:102770.
33. Wen-de W, Min L, Ming C, et al. Development of a colloidal gold immunochromatographic strip for rapid detection of *Streptococcus agalactiae* in tilapia. *Biosens Bioelectron*. 2017;91:66–69.
34. Wang Z, Zheng Z, Hu H, et al. A point-of-care selenium nanoparticle-based test for the combined detection of anti-SARS-CoV-2 IgM and IgG in human serum and blood. *Lab Chip*. 2020;20(22):4255–4261.
35. Quesada-González D, Merkoçi A. Nanoparticle-based lateral flow biosensors. *Biosens Bioelectron*. 2015;73:47–63.
36. Chen C, Hu H, Li X, et al. Rapid detection of anti-SARS-CoV-2 antibody using a selenium nanoparticle-based lateral flow immunoassay. *IEEE Trans Nanobiosci*. 2022;21(1):37–43.
37. Wang Z, Zhi D, Zhang H, et al. Synthesis of selenium nanoparticles suitable for melamine detection using test strips. *Nanosci Nanotec Let*. 2015;7(8):617–622.
38. Liu X, Yuan Z, Tang Z, et al. Selenium-driven enhancement of synergistic cancer chemo/radiotherapy by targeting nanotherapeutics. *Biomater Sci*. 2021;9(13):4691–4700.
39. Cole LA. Immunoassay of human chorionic gonadotropin, its free subunits, and metabolites. *Clin Chem*. 1997;43:2233–2243.

## International Journal of Nanomedicine

Dovepress

### Publish your work in this journal

The International Journal of Nanomedicine is an international, peer-reviewed journal focusing on the application of nanotechnology in diagnostics, therapeutics, and drug delivery systems throughout the biomedical field. This journal is indexed on PubMed Central, MedLine, CAS, SciSearch®, Current Contents®/Clinical Medicine, Journal Citation Reports/Science Edition, EMBase, Scopus and the Elsevier Bibliographic databases. The manuscript management system is completely online and includes a very quick and fair peer-review system, which is all easy to use. Visit <http://www.dovepress.com/testimonials.php> to read real quotes from published authors.

Submit your manuscript here: <https://www.dovepress.com/international-journal-of-nanomedicine-journal>